

10-31-2009

# Androgens Regulate Prostate Cancer Cell Growth via an AMPK-PGC-1 $\beta$ -Mediated Metabolic Switch

Jayantha B. B. Tennakoon

*Center for Nuclear Receptors and Cell Signaling, Department of Biology and Biochemistry*

Yan Shi

*Center for Nuclear Receptors and Cell Signaling, Department of Biology and Biochemistry*

Jenny J. Han

*Center for Nuclear Receptors and Cell Signaling, Department of Biology and Biochemistry*

Efrosini Tsouko

*Center for Nuclear Receptors and Cell Signaling, Department of Biology and Biochemistry*

Mark A. White

*Center for Nuclear Receptors and Cell Signaling, Department of Biology and Biochemistry*

*See next page for additional authors*

Follow this and additional works at: [https://digitalcommons.fiu.edu/all\\_faculty](https://digitalcommons.fiu.edu/all_faculty)

---

## Recommended Citation

Tennakoon, Jayantha B. B.; Shi, Yan; Han, Jenny J.; Tsouko, Efrosini; White, Mark A.; Burns, Alan R.; Zhang, Aijun; Xia, Xuefeng; Ilkayeva, Olga R.; Xin, Li; Ittmann, Michael M.; Rick, Ferenc G.; Schally, Andrew V.; and Frigo, Daniel E., "Androgens Regulate Prostate Cancer Cell Growth via an AMPK-PGC-1 $\beta$ -Mediated Metabolic Switch" (2009). *All Faculty*. 51.  
[https://digitalcommons.fiu.edu/all\\_faculty/51](https://digitalcommons.fiu.edu/all_faculty/51)

---

**Authors**

Jayantha B. B. Tennakoon, Yan Shi, Jenny J. Han, Efrosini Tsouko, Mark A. White, Alan R. Burns, Aijun Zhang, Xuefeng Xia, Olga R. Ilkayeva, Li Xin, Michael M. Ittmann, Ferenc G. Rick, Andrew V. Schally, and Daniel E. Frigo



Published in final edited form as:

*Oncogene*. 2014 November 6; 33(45): 5251–5261. doi:10.1038/onc.2013.463.

## Androgens Regulate Prostate Cancer Cell Growth via an AMPK- PGC-1 $\alpha$ -Mediated Metabolic Switch

Jayantha B. Tennakoon<sup>1</sup>, Yan Shi<sup>1</sup>, Jenny J. Han<sup>1</sup>, Efrosini Tsouko<sup>1</sup>, Mark A. White<sup>1</sup>, Alan R. Burns<sup>2</sup>, Aijun Zhang<sup>3</sup>, Xuefeng Xia<sup>3</sup>, Olga R. Ilkayeva<sup>4</sup>, Li Xin<sup>5,6,7</sup>, Michael M. Ittmann<sup>6,7,8</sup>, Ferenc G. Rick<sup>9,10</sup>, Andrew V. Schally<sup>9,11,12,13</sup>, and Daniel E. Frigo<sup>1,3</sup>

<sup>1</sup>Center for Nuclear Receptors and Cell Signaling, Department of Biology and Biochemistry

<sup>2</sup>College of Optometry, University of Houston, Houston, TX, USA

<sup>3</sup>Center for Genomic Medicine, Houston Methodist Research Institute, Houston, TX, USA

<sup>4</sup>Department of Pharmacology and Cancer Biology, Duke University Medical Center, Durham, NC, USA

<sup>5</sup>Departments of Molecular and Cellular Biology, Baylor College of Medicine, Houston, TX, USA

<sup>6</sup>Pathology and Immunology, Baylor College of Medicine, Houston, TX, USA

<sup>7</sup>Dan L. Duncan Cancer Center, Houston, TX, USA

<sup>8</sup>Michael E. DeBakey Veterans Affairs Medical Center, Houston, TX, USA

<sup>9</sup>Veterans Affairs Medical Center and South Florida VA Foundation for Research and Education, Miami, FL, USA

<sup>10</sup>Department of Urology, Florida International University, Herbert Wertheim College of Medicine, Miami, FL, USA

<sup>11</sup>Department of Pathology, University of Miami, Miller School of Medicine, Miami, FL, USA

<sup>12</sup>Hematology/Oncology, University of Miami, Miller School of Medicine, Miami, FL, USA

<sup>13</sup>Endocrinology, Department of Medicine, University of Miami, Miller School of Medicine, Miami, FL, USA

### Abstract

Prostate cancer is the most commonly diagnosed malignancy among men in industrialized countries, accounting for the second leading cause of cancer-related deaths. While we now know that the androgen receptor (AR) is important for progression to the deadly advanced stages of the disease, it is poorly understood what AR-regulated processes drive this pathology. Here, we demonstrate that AR regulates prostate cancer cell growth via the metabolic sensor 5'-AMP-

---

Users may view, print, copy, download and text and data- mine the content in such documents, for the purposes of academic research, subject always to the full Conditions of use: [http://www.nature.com/authors/editorial\\_policies/license.html#terms](http://www.nature.com/authors/editorial_policies/license.html#terms)

Corresponding Author: Daniel E. Frigo, Center for Nuclear Receptors and Cell Signaling, University of Houston, 3605 Cullen Blvd, Houston, TX 77204. Tel: 832-842-8824. Fax: 713-743-0634. E-mail: [frigo@uh.edu](mailto:frigo@uh.edu).

**Conflict of Interest:** The authors declare no conflict of interest.

Supplementary Information accompanies the paper on the *Oncogene* website (<http://www.nature.com/onc>)

activated protein kinase (AMPK), a kinase that classically regulates cellular energy homeostasis. In patients, activation of AMPK correlated with prostate cancer progression. Using a combination of radiolabeled assays and emerging metabolomic approaches, we also show that prostate cancer cells respond to androgen treatment by increasing not only rates of glycolysis, as is commonly seen in many cancers, but also glucose and fatty acid oxidation. Importantly, this effect was dependent on androgen-mediated AMPK activity. Our results further indicate that the AMPK-mediated metabolic changes increased intracellular ATP levels and peroxisome proliferator-activated receptor gamma coactivator 1-alpha (PGC-1 $\alpha$ )-mediated mitochondrial biogenesis, affording distinct growth advantages to the prostate cancer cells. Correspondingly, we used outlier analysis to determine that PGC-1 $\alpha$  is overexpressed in a subpopulation of clinical cancer samples. This was in contrast to what was observed in immortalized benign human prostate cells and a testosterone-induced rat model of benign prostatic hyperplasia. Taken together, our findings converge to demonstrate that androgens can co-opt the AMPK-PGC-1 $\alpha$  signaling cascade, a known homeostatic mechanism, to increase prostate cancer cell growth. The current study points to the potential utility of developing metabolic-targeted therapies directed towards the AMPK-PGC-1 $\alpha$  signaling axis for the treatment of prostate cancer.

### Keywords

androgen receptor; prostate cancer; AMP-activated protein kinase; peroxisome proliferator-activated receptor  $\gamma$  coactivator 1 $\alpha$ ; metabolism

---

### Introduction

Since the 1920's, it has been known that cancer cells possess the unique ability to alter their metabolism and, as such, are distinguishable from benign cells.<sup>1</sup> However, it was only in the past decade that the reprogramming of energy metabolism has been acknowledged as one of the true emerging hallmarks of cancer.<sup>2</sup> Interestingly, while the majority of metabolic cancer research focuses on the role of glycolysis, it has recently become apparent that the tricarboxylic acid (TCA) cycle and oxidative phosphorylation (OXPHOS) also play major roles in many types of cancers including prostate cancer.<sup>3-6</sup> Both the genetic deletion or pharmacological inhibition of key steps in the TCA cycle and/or OXPHOS can block cancer cell growth *in vitro* and disease progression *in vivo*.<sup>7-10</sup> Further, metabolic signatures of the TCA cycle and OXPHOS correlate with cancer progression and unfavorable outcomes.<sup>9,11-17</sup> Also, 2-<sup>18</sup>F-fluoropropionic acid and <sup>11</sup>C-acetate, new tracers being used for positron emission tomography (PET) imaging, are more sensitive detectors of prostate cancer than the glycolysis marker <sup>18</sup>F-fluorodeoxyglucose.<sup>18-21</sup> These data indicate that prostate cancers can exhibit unique metabolic profiles. What is not understood is specifically how androgen receptor (AR)-signaling, elevated in 100% of metastatic prostate cancers,<sup>22</sup> impacts cellular metabolism and what role this plays in disease progression.

Prostate cancers express the AR and rely on androgens for growth and survival.<sup>23</sup> Consequently, androgen ablation therapies are the standard of care for late-stage disease. While patients with advanced prostate cancer initially respond favorably to androgen ablation therapy, most experience a relapse of the disease within 1-2 years. Following this

castration-resistant relapse, patients have limited treatment options. Although the hormone-refractory disease is unresponsive to androgen-deprivation, AR-regulated signaling pathways remain active and are necessary for cancer progression.<sup>23,24</sup> Thus, both AR itself and the processes downstream of the receptor remain viable targets for therapeutic intervention.

The master metabolic regulator AMP-activated protein kinase (AMPK) governs overall cellular homeostasis by modulating the use of sugars, fats and/or proteins as sources of cellular fuel. Recent work from our laboratory has demonstrated that androgens increase cellular migration and invasion through the direct upregulation of Ca<sup>2+</sup>/calmodulin-dependent protein kinase kinase  $\beta$  (CaMKK $\beta$ ) and subsequent threonine-172 (refers to threonine-183/172 of the AMPK $\alpha$  1/AMPK $\alpha$ 2 isoforms, respectively) phosphorylation/activation of the catalytic subunit of AMPK.<sup>25</sup> Later, two more independent groups confirmed our CaMKK $\beta$  findings *in vitro* and in multiple clinical cohorts and suggested CaMKK $\beta$  also promotes glycolytic flux.<sup>26,27</sup> Correspondingly, Park et al demonstrated that levels of the serine-79 phosphorylated form of acetyl-CoA carboxylase (ACC), a direct target of AMPK, are increased in clinical prostate cancer samples.<sup>28</sup> Because of the importance of androgen signaling in prostate cancer, and the increasing evidence from other laboratories as well as our own that suggest AMPK may have an oncogenic role in certain cancer contexts,<sup>25-31</sup> we wanted to determine whether AR signaling promoted prostate cancer cell growth in part through AMPK signaling. Further, given AMPK's role as a central regulator of cellular metabolism, we also wanted to determine whether AR-mediated AMPK signaling influenced prostate cancer cell biology through additional mechanisms beyond those classically attributed to cancer (i.e. glycolysis).

## Results

### AMPK is required for androgen-mediated prostate cancer cell growth

Our previous work identified a role for CaMKK $\beta$ -AMPK signaling in AR-mediated prostate cancer cell migration and invasion.<sup>25</sup> Subsequent studies confirmed AR's regulation of CaMKK $\beta$  in prostate cancer and demonstrated its additional importance in regulating prostate cancer growth both *in vitro* and *in vivo*.<sup>26,27</sup> Additionally, Massie et al showed that CaMKK $\beta$  augmented cell growth in part through increased glucose metabolism, an effect they suggested may be mediated through AMPK.<sup>27</sup> In that study, the role of AMPK was inferred from experiments that used pharmacological AMP mimetics that, while known activators of AMPK, cause cellular stress and therefore, may indirectly affect cell growth. Because of these and other known pleiotropic effects of various AMPK modulators (ex. compound C blocks AR activity<sup>25</sup>), we wanted to confirm a direct role for AMPK in AR-mediated prostate cancer cell growth using molecular approaches. To do so, we blocked AMPK activity using siRNAs targeting three separate regions of the predominant catalytic subunit of AMPK found in the prostate.<sup>25</sup> In both LNCaP and VCaP human prostate cancer cells, siRNA-mediated knockdown of AMPK $\alpha$ 1 decreased the levels of both total AMPK $\alpha$  and the threonine-172/activation loop phosphorylated form of AMPK $\alpha$ , indicating blocked AMPK activity (Figs. 1A and B). Importantly, all three siRNAs targeting AMPK significantly inhibited R1881 (a synthetic androgen)-mediated prostate cancer cell growth in

both cell types (Figs. 1C and D), an effect that was observed by three days (Supplemental Fig. S1).

### **Phosphorylated/Activated AMPK correlates with prostate cancer progression in patients**

A tissue microarray (TMA) containing benign and primary cancer tissues was examined by immunohistochemistry (IHC) to determine if phospho-AMPK (Thr172), the activating phosphorylation site, was increased in prostate cancer (Fig. 2). Staining of p-AMPK in the TMA was quantified using a multiplicative staining index of intensity (0-3) and extent (0-3) of staining, which yields a 10-point staining index (0-9) as described previously.<sup>32-34</sup> In benign tissues, weak staining (score 3) was observed in luminal cell cytoplasm in some tissues, with other tissues showing no staining. Occasional tissues showed moderate staining (score 6). In all cases, staining was uniform within each core. Variable cytoplasmic staining was seen in the cancer cells in different tissues ranging from no staining to strong staining (score 9). Overall, staining was significantly stronger in cancer (Fig. 2A). Occasional weak staining was seen in stromal cells in both benign and cancer tissues. Of note, higher p-AMPK staining was significantly correlated with biochemical (PSA) recurrence following radical prostatectomy (non-recurrent  $3.2 \pm 0.4$  (mean  $\pm$  SEM,  $n=29$ ) versus recurrent  $4.6 \pm 0.4$  ( $n=32$ ))(Fig. 2B). The p-AMPK IHC score was not correlated with pathological variables such as Gleason score or disease stage at the time of surgery.

### **Androgens promote both glycolysis and OXPHOS**

Given AMPK's role as a master regulator of metabolism and its regulation by AR in the prostate, we next asked what effects androgens had on prostate cancer cell metabolism. To quantitate glycolytic rates, we measured the extracellular acidification rate (ECAR) in prostate cancer cells following treatment with R1881. In both LNCaP and VCaP cells, R1881 increased glycolysis in a dose-dependent manner (Figs. 3A-C). Consistent with what has previously been shown,<sup>35</sup> the dose response was unaffected by various modulators of mitochondrial function (Fig. 3C), highlighting the cytoplasmic nature of glycolysis. Interestingly, simultaneous measurement of the oxygen consumption rate (OCR) indicated that androgens also increased oxygen consumption in a dose-dependent manner (Figs. 3D-F). This androgen-mediated increase in OCR was dependent on mitochondrial function as combined treatment of rotenone and antimycin, inhibitors of mitochondrial respiration, collapsed the response (Fig. 3F). The increased oxygen consumption indicated androgens promote metabolism not only through glycolysis, but also through the TCA cycle. In support of this, we used MS/MS to show that androgens increased intracellular levels of acetyl-CoA, the entry molecule for the TCA cycle (Fig. 3G). Importantly, GC/MS was used to demonstrate that androgens also increased the levels of all TCA cycle intermediates tested, suggesting that acetyl-CoA is not only entering the TCA cycle, but also metabolized completely through it (Fig. 3H). These data are in contrast to Massie et al who found that androgen treatment increased citrate but not succinate levels nor oxygen consumption.<sup>27</sup> To verify whether complete oxidation was occurring, we used a radiolabeled CO<sub>2</sub> trap assay to demonstrate that androgens increase complete glucose oxidation (Fig. 3I; Supplemental Fig. S2A). These results indicate that androgens promote the uptake and metabolism of radiolabeled glucose through at least  $\sim 1.5$  turns of the TCA cycle prior to the radiolabeled 1-carbon of glucose being released in the form of CO<sub>2</sub>.

While the majority of metabolic cancer research focuses on the role of glucose, recently several groups have demonstrated an important role for fatty acid metabolism in prostate cancer.<sup>18,36-38</sup> Correspondingly, in our hands,  $\beta$ -oxidation was required for maximal androgen-mediated prostate cancer cell growth as co-treatment with etomoxir, an inhibitor of carnitine palmitoyltransferase I—the rate-limiting step of  $\beta$ -oxidation, suppressed androgen-mediated LNCaP growth (Fig. 3J). We therefore tested whether androgens could also promote fatty acid oxidation in prostate cancer cells by tracking the metabolism of radiolabeled fatty acids. Treatment of either LNCaP (Figs. 3K-L) or VCaP (Supplemental Figs. S2B and C) cells with increasing concentrations of androgens promoted, in a dose-dependent manner, the complete oxidation of both the saturated fatty acid palmitate and the monounsaturated fatty acid oleate, two of the most common  $\beta$ -oxidation substrates. Importantly, this correlates with previous clinical data demonstrating the increased metabolism of both sugars and fats in aggressive metastatic prostate cancers compared to localized tumors.<sup>39</sup> Taken together, these findings indicate that androgens increase both glycolysis (sugars) and OXPHOS (sugars and fats) in prostate cancer cells.

### **AMPK is required for androgen-mediated OXPHOS**

AMPK is a positive regulator of OXPHOS. Given that AMPK is required for androgen-mediated prostate cancer cell growth (Fig. 1), we next wanted to determine whether the androgen-mediated increase in OXPHOS was mediated by AMPK. To do this, we used two different approaches. First, we demonstrated in both LNCaP and VCaP cells that molecular knockdown of AMPK decreased androgen-mediated oxygen consumption (Figs. 4A and B). Second, knockdown of AMPK significantly inhibited the androgen-mediated oxidation of radiolabeled glucose (Figs. 4C and D), palmitate (Figs. 4E and F) and oleate (Figs. 4G and H).

One of the major functions of mitochondrial OXPHOS is to generate ATP. We therefore wanted to determine whether the androgen-mediated OXPHOS indeed led to an increase in intracellular ATP levels and hence, helped fulfill the cancer cell's bioenergetic demands. Using a luciferase-based ATP assay, we determined that R1881 increased intracellular ATP levels in a dose-dependent manner (Fig. 5A). This R1881-mediated increase in ATP levels was blocked by transfection with the siRNAs targeting AMPK (Fig. 5B). These results indicate that androgens increase mitochondrial function through AMPK.

### **Androgen-mediated AMPK signaling increases PGC-1 $\alpha$ levels, which are elevated in a subpopulation of prostate cancers**

Our data indicate that androgens increase overall mitochondrial function. However, the mechanism for this effect was still unknown. One of the known targets of AMPK is peroxisome proliferator-activated receptor gamma coactivator 1-alpha (PGC-1 $\alpha$ ), a transcriptional coactivator that is a master regulator of mitochondrial biogenesis and function.<sup>40</sup> Therefore, we tested whether androgens could increase PGC-1 $\alpha$  levels in prostate cancer cells. Androgens, starting at 100 pM, significantly increased PGC-1 $\alpha$  protein levels in a dose-dependent manner in both LNCaP (Fig. 6A) and VCaP (Fig. 6B) prostate cancer cells. Using qPCR, we found that increasing concentrations of R1881 could also increase PGC-1 $\alpha$  mRNA levels in LNCaP (Fig. 6C) and VCaP (Fig. 6D) cells after a 72

hour treatment. This induction was not seen following a 24-hour treatment (Supplemental Fig. S3). Interestingly, despite the robust expression of AR, androgens did not significantly alter PGC-1 $\alpha$  levels in a stepwise genetic model of prostate cancer progression<sup>41</sup> (Supplemental Fig. S4). This is not completely surprising given a) the heterogeneous nature of prostate cancer and b) in culture, none of these cells display an androgen-mediated growth response.<sup>41</sup> However, using a hormone-inducible rat model of benign prostatic hyperplasia (BPH), we observed that while testosterone treatment increased prostate growth,<sup>42,43</sup> it did not increase PGC-1 $\alpha$  protein levels (Supplemental Fig. S5). This is in contrast to the increased PGC-1 $\alpha$  levels observed in tumors derived from the dorsolateral lobes of the well-characterized Pb-Cre, Pten<sup>f/f</sup> mouse model of prostate cancer<sup>44</sup> (Supplemental Fig. S6) or the Pb-Myc mouse model of prostate cancer<sup>45</sup>. Additionally, comparison of parental LNCaP cells to their castration-resistant prostate cancer (CRPC)-derivative C4-2 cell line (derived from castration-resistant selection in xenografts) demonstrates that p-AMPK and, accordingly, PGC-1 $\alpha$  levels are markedly elevated in the CRPC C4-2 model relative to parental LNCaPs (Fig. 6E). Xenograft-derived LAPC9 tumors that were either propagated in intact mice or serially propagated for 13 generations in castrated mice revealed that, despite decreased AR levels, PGC-1 $\alpha$  levels are maintained and surprisingly, total AMPK and, subsequently, p-AMPK levels are increased in the CRPC model (Fig. 6E). While this is the first time we had observed changes in total AMPK levels, it is important to note that AMPK $\alpha$ 1/*PRKAA1* (the predominant isoform of the catalytic subunit of AMPK expressed in the prostate<sup>25</sup>) levels correlate with poor prognosis in patients (Supplemental Fig. S7).<sup>22</sup> These findings corroborate the clinical p-AMPK TMA data shown in Figure 2. Taken together, our results suggest that AMPK-PGC-1 $\alpha$  signaling correlates with cancer growth and can be indirectly regulated by AR.

To test whether AMPK was responsible for the androgen-mediated increase in PGC-1 $\alpha$  levels, we used the same siRNAs targeting AMPK described in Figure 1 to determine what effects they had on both basal and androgen-mediated PGC-1 $\alpha$  levels (Figs. 6F and G; Supplemental Fig. S8). In LNCaP and VCaP cells, knockdown of AMPK led to a significant decrease in both PGC-1 $\alpha$  protein (Fig. 6F; Supplemental Figs. S8A and B) and mRNA (Fig. 6G; Supplemental Fig. S8C) levels, demonstrating a clear requirement for AMPK in AR-mediated induction of PGC-1 $\alpha$ . Finally, stable knockdown of PGC-1 $\alpha$  suppressed prostate cancer cell growth/survival over three days roughly 40% in LNCaP cells (Supplemental Fig. S8D) and, importantly, 50% in the CRPC C4-2 model (Fig. 6H), highlighting a potential role for PGC-1 $\alpha$  in the advanced disease.

Given that PGC-1 $\alpha$  levels were increased in multiple models of prostate cancer, we next determined if its expression correlated with prostate cancer in patients. Analysis of clinically annotated prostate cancer data sets accessible through Oncomine revealed that PGC-1 $\alpha$  expression was significantly higher in cancers compared to controls (Supplemental Fig. S9A).<sup>46</sup> While this increase was significant, it was derived from a study with a modest cohort size (19 patients). Because of the high degree of heterogeneity in prostate cancer, we asked whether PGC-1 $\alpha$  levels might be elevated in a subset of cancers. Using outlier analysis, we found that PGC-1 $\alpha$  was indeed overexpressed in a subpopulation of prostate cancers in multiple clinical cohorts (Supplemental Fig. S9B).<sup>46-50</sup> To better clinically define



this subset of patients, we took advantage of the emerging well-annotated datasets available from The Cancer Genome Atlas. Here, PGC-1 $\alpha$  is significantly overexpressed in ~5% of prostate cancer patients (no patients had significantly decreased expression). These patients exhibited clinical pathologic T stages from T2c-T3b and Gleason scores from 7-9 with a mean of 7.4. Interestingly, patients from this subpopulation are initially diagnosed with prostate cancer significantly earlier ( $56.0 \pm 1.5$  years old versus  $60.2 \pm 0.5$  years for the average prostate cancer patient).

### **AR-AMPK-PGC-1 $\alpha$ signaling promotes mitochondrial biogenesis and cell growth**

Mitochondrial function is essential for both basic cellular homeostasis as well as increased cell growth.<sup>51</sup> Given recent studies that suggest a previously underappreciated role for mitochondrial function in cancer,<sup>3-17</sup> we decided to test whether androgens could increase mitochondrial biogenesis in prostate cancer cells. Using transmission electron microscopy (TEM), we found that LNCaP cells treated for 72 hours had significantly more mitochondria (Fig. 7A). To test whether the AMPK-mediated induction of PGC-1 $\alpha$  promoted androgen-mediated mitochondrial biogenesis in a more unbiased manner, we used confocal microscopy and subsequent image analysis to quantitatively assess if AMPK and/or PGC-1 $\alpha$  were required (Figs 7B-D; Supplemental Figs. S10 and 11). Using our two most efficacious siRNAs targeting AMPK<sup>25</sup> or PGC-1 $\alpha$  (Supplemental Fig. S11), siRNA-mediated knockdown of either AMPK or PGC-1 $\alpha$  significantly decreased mitochondrial volume in LNCaP and VCaP cells (Figs. 7B-D; Supplemental Figs. S10 and 11). Similar to knockdown of AMPK (Figs. 1 and 4), molecular inhibition of PGC-1 $\alpha$  also blocked androgen-mediated OXPHOS (Fig. 7E) and, in concordance with what others have reported,<sup>52</sup> prostate cancer cell growth (Fig. 7F), an effect that was observed by three days (Supplemental Figs. S11C and D). However, it should be noted that unlike what has previously been reported,<sup>52</sup> in our hands PGC-1 $\alpha$  did not feedback to further potentiate AR activity (Supplemental Fig. S12). Collectively, these results indicate a role for a more linear AR-AMPK-PGC-1 $\alpha$  signaling cascade in prostate cancer cell growth.

### **Discussion**

While much of the research on cancer metabolism has historically focused on glycolysis, it is now becoming apparent that not all cancers depend solely on glycolytic metabolism. Prostate cancer, in particular, appears to utilize other processes to fulfill its metabolic demands. Accordingly, the glycolysis marker <sup>18</sup>F-fluorodeoxyglucose is a relatively poor PET imaging marker for prostate cancer.<sup>18,19</sup> Conversely, labeled fatty acid and acetate analogs, which can be shuttled to fatty acid metabolism and/or enter the TCA cycle, have shown more promising results.<sup>18,20,21</sup> Interestingly, zinc and citrate levels are higher in normal prostate epithelial cells than any other cell in the body. When prostate epithelial cells become cancerous, they are uniquely characterized by decreased zinc and citrate levels, which parallels with increased citrate oxidation and OXPHOS.<sup>5,6</sup> Further, mitochondrial biogenesis, TCA cycle and OXPHOS signatures correlate with unfavorable outcomes in prostate cancer as well as other cancer types.<sup>3,11,13,15,16,53-56</sup> Inhibition of mitochondrial function/OXPHOS results in cell death or cell cycle arrest in multiple cancer types.<sup>8-10,17</sup>

Thus, while glycolysis is a major metabolic pathway in cancer, mitochondrion-mediated functions still appear essential for many cancer cell types including prostate.

The findings above suggest that mitochondria could be an important target for various oncogenic and tumor suppressor signaling cascades. Correspondingly, the telomerase oncogene promotes mitochondrial biogenesis and prostate cancer bone metastasis while the tumor suppressor p53 suppresses PGC-1-mediated mitochondrial biogenesis.<sup>13,54,55</sup> Our data presented here indicate that AR signaling also increases AMPK-PGC-1-mediated mitochondrial biogenesis and prostate cancer cell growth (Fig. 7). This raises the question of how mitochondrial biogenesis contributes to cell growth. One obvious possibility is that rapidly dividing cells have high bioenergetic demands. By increasing the mitochondrial content of the cell, androgens also increased the intracellular levels of ATP (Fig. 5). Recently, however, it has been determined that the level of building blocks (ex. amino acids for protein production, etc), rather than the level of ATP, may be the major rate-limiting factor for rapidly dividing cells.<sup>4</sup> As such, making sure a high level of TCA cycle intermediates are maintained, a process termed anaplerosis, would be essential as the TCA cycle serves as a central metabolic hub from which many of the cellular building blocks are derived (Fig. 8). Our findings that androgens increase TCA cycle intermediate levels and promote the metabolism of glucose and fatty acids through the TCA cycle (Fig. 3), suggest that AR signaling is also anaplerotic. Current studies are ongoing to determine where substrates are ultimately shuttled following androgen treatment.

The data presented here indicate that AMPK signaling is required for androgen-mediated prostate cancer cell growth and is elevated in prostate cancer and, importantly, recurrent prostate cancer (Figs. 1 and 2). To date, the role of AMPK in cancer has been enigmatic. We (data not shown), and others,<sup>57</sup> have demonstrated that 5-aminoimidazole-4-carboxamide 1- $\beta$ -D-ribo-furanoside (AICAR) and the antidiabetic drugs metformin and rosiglitazone, which all activate AMPK, also inhibit prostate cancer cell growth. Conversely, while Massie et al also found that metformin inhibited LNCaP cell growth, they showed AICAR increased LNCaP cell growth in the presence or absence of androgens. Additionally, AICAR was able to rescue the growth inhibitory effects of either CaMKK $\beta$  RNAi knockdown or STO-609 (CaMKK antagonist) treatment.<sup>27</sup> Further, AMPK has been shown to be activated in clinical prostate cancer samples and inhibition of its activity by compound C or siRNAs targeting AMPK blocks cancer cell growth (Figs. 1 and 2).<sup>28</sup> These discrepancies may be due to the pleiotropic effects of the various small molecules being used to modulate AMPK activity. For example, AICAR functions by inducing cellular stress. One of the results of this increased cellular stress is the activation of AMPK. However, the widespread increase in cellular stress may undoubtedly function to inhibit cellular growth through other stress signaling pathways. Alternatively, the pro-growth effects of AMPK may, similar to many signaling cascades, occur within a defined window of activity where some controlled AMPK activity promotes a metabolic shift that enhances cell growth but too much AMPK activity signals stress and subsequent cell cycle arrest.

In prostate cancer cells, androgens increase PGC-1 $\alpha$  protein and mRNA levels (Figs. 6A-D). While we know AMPK is required for this PGC-1 $\alpha$  regulation (Figs. 6F and G; Supplementary Fig. S8), we still do not understand the exact mechanism. Previously, Bruce

Spiegelman's laboratory demonstrated that AMPK increases both PGC-1 $\alpha$  protein and mRNA levels in skeletal muscle.<sup>40</sup> In that study, they found that AMPK directly phosphorylates PGC-1 $\alpha$  on threonine-177 and serine-538. These phosphorylation events then increase the activity of PGC-1 $\alpha$  protein on its own promoter, increasing its expression through a mechanism that may involve the transcription factors GATA-4 and Upstream Stimulatory Factor-1.<sup>58</sup> Hence, the AR-AMPK mediated increase in PGC-1 $\alpha$  protein and mRNA levels may occur through the direct posttranslational phosphorylation of PGC-1 $\alpha$  protein by AMPK and subsequent positive feedback expression of the *PPARGCIA* gene.

Our data correlate with recent findings that indicate PGC-1 $\alpha$  signaling is upregulated in endometrial cancer,<sup>12</sup> drives breast cancer tumor growth *in vivo*,<sup>59</sup> and *Pgc1 $\alpha$ -/-* mice are resistant to chemically-induced models of colon and liver cancer.<sup>7</sup> Correspondingly, Shiota et al also demonstrated that PGC-1 $\alpha$  was essential for prostate cancer cell growth.<sup>52</sup> Interestingly, in that study, PGC-1 $\alpha$  was shown to function as a coactivator of AR. In our hands, we did not observe this effect (Supplemental Fig. S12). Thus, our current data indicate AR, via AMPK, increases PGC-1 $\alpha$  levels in a more linear manner (Fig. 8). Whether AMPK and PGC-1 $\alpha$  promote cancer cell growth through additional mechanisms remains to be determined. Hence, while AMPK-PGC-1 $\alpha$  signaling promotes prostate cancer cell growth in part through increasing mitochondrial function (known because inhibition of mitochondrial function decreases cell growth/survival (Fig. 3J)<sup>10</sup>), AMPK-PGC-1 $\alpha$  signaling may also enhance prostate cancer cell growth through additional, mitochondrion-independent mechanisms (ex. increasing cyclin D levels, etc). This could also help explain why knockdown of PGC-1 $\alpha$  had a more dramatic effect on cell growth (Fig. 7F; Supplemental Figs. S11C and D) than it did on mitochondrial biogenesis (Figs. 7B-D; Supplemental Figs. S10 and 11). The more modest effects on mitochondrial biogenesis were likely due to the suboptimal efficacy of our PGC-1 $\alpha$  -targeting siRNAs (Supplemental Fig. S11). Conversely, the dramatic effect of molecular PGC-1 $\alpha$  inhibition on growth suggests that PGC-1 $\alpha$  may potentiate androgen-mediated prostate cancer cell growth through additional mechanisms. As a result, the modest inhibition of a single protein, PGC-1 $\alpha$ , would result in pronounced overall growth effects.

Collectively, the data presented here suggest that AR signaling promotes AMPK-PGC-1 $\alpha$  -mediated mitochondrial biogenesis and cell growth. This is important because while AR's role in prostate cancer has been well established, the mechanisms by which AR manifests its biological actions and how these are dysregulated during disease progression are poorly understood. As a result, it is essential to identify the AR signaling networks that truly drive disease progression. Our understanding of these signaling pathways will ultimately yield new therapeutic targets. Hence, as our data indicate, modulators of mitochondrial function may offer new therapeutic avenues for AR-driven prostate cancer.

## Materials and Methods

### Reagents and standard biochemical and molecular approaches

More detailed descriptions of reagents, cell culture, siRNA transfections, Western blot analyses, proliferation assays, radiolabeled CO<sub>2</sub> trap assays, ATP assays, real-time PCR

analyses, microscopy, viability assays and reporter gene assays are provided in the Supplementary Information.

### Human tissues and tissue microarray analysis

Prostate cancer TMAs were constructed using tissues collected after radical prostatectomy with informed consent by the Baylor College of Medicine Human Tissue Acquisition and Pathology Core under an IRB-approved protocol. The arrays were 1 mm cores of 80 cancers and matched benign tissues with equal numbers of cases with and without biochemical recurrence. Arrays stained with anti-phospho-AMPK antibody were carried out as described in the Supplementary Material and quantitated using a multiplicative staining index of intensity (0-3) and extent (0-3) of staining yielding a 10-point staining index (0-9) as described in previous publications.<sup>32-34</sup> Some cancer cores could not be scored due to exhaustion of tumor in the core and likewise in some cores no benign epithelium was present. Overall 61 cancers and 65 benign tissues could be scored. Scoring was performed without knowledge of the corresponding clinical and pathological variables.

### Extracellular acidification rate (ECAR) and oxygen consumption rate (OCR) measurements

ECAR, reflective of the rate of glycolysis, and OCR, reflective of the rate of OXPHOS, were measured using a Seahorse Bioscience XF24 analyzer (North Billerica, MA, USA). Cells were plated at 30,000 cells/well in Seahorse XF24 plates coated with BD Cell-Tak (BD Biosciences) and incubated for 48 hours. For R1881 dose response experiments, the cells were then treated for 72 hours. For knockdown experiments, cells were transfected with indicated siRNAs overnight prior to treatment. For ECAR and OCR measurements in the presence of inhibitors (oligomycin-1.3  $\mu$ M; Carbonyl cyanide 4-(trifluoromethoxy)phenylhydrazone (FCCP)-1  $\mu$ M; rotenone-1  $\mu$ M; antimycin A-1  $\mu$ M), the samples were treated with R1881 and then incubated for 72 hours. During the initial/basal phase of assaying no inhibitors were present. Thereafter at respective time points inhibitor-containing media were sequentially injected to the assay wells through automated instrument ports. Data were normalized to cell numbers using the DNA content assay described in the Supplementary Information.

### Metabolic profiling

Measurements of intracellular acetylcarnitine levels, which are reflective of acetyl-CoA levels, and organic acid/TCA cycle intermediates were performed using tandem mass spectrometry (MS/MS) or gas chromatography/mass spectrometry (GC/MS) as previously described.<sup>60</sup>

### Animal studies

ARR2PB-Cre (Pb-Cre) transgenic mice<sup>61</sup> were from Dr. Fen Wang (Texas A&M Health Science Center, Houston, TX, USA). Pten<sup>ff</sup> mice<sup>44</sup> were from Dr. Hong Wu (University of California Los Angeles, CA, USA). Breeding, crosses, dissociation of prostate tumors and RNA isolation were performed using previously described approaches.<sup>62</sup>

Adult male Wistar rats (Charles River Laboratories, Wilmington, MA, USA) between 10 and 11 weeks of age were used as a testosterone-induced model of BPH as previously

described. Housing conditions, treatments and isolation of ventral prostates were previously described.<sup>42,43</sup> All animals remained healthy throughout the experiments. Animal care was in accordance with institutional guidelines and complied with NIH policy.

### Statistical analysis

Two-sample comparisons were performed using Student's *t*-tests. Multiple comparisons were performed using a one-way ANOVA and *post-hoc* Dunnett's test with GraphPad Prism, Version 4 (GraphPad Software, La Jolla, CA, USA). TMA staining intensity groups were compared using Mann-Whitney tests. Kaplan-Meier curves were compared using a log-rank test. Significant changes were determined at the  $P < 0.05$  level unless otherwise noted.

### Supplementary Material

Refer to Web version on PubMed Central for supplementary material.

### Acknowledgments

We thank members of the Frigo Laboratory for technical advice, helpful suggestions and critical comments on this study and manuscript. We also thank Paul Landry for his assistance with Amira and mitochondrial volume measurements, the Duke University Department of Pathology's Electron Microscopy Core for help with TEM; Drs. Dean Tang, Geoffrey Girnun and Thomas Westbrook for generously providing the LAPC9-derived tumors, shPGC-1 $\alpha$  constructs and pINDUCER22, respectively; Drs. Timothy Koves and Pradip Saha for advice on the CO<sub>2</sub> trap assays; Dr. Christopher Newgard for help with the metabolomics; and Drs. Sean McGuire and Kevin Phillips for critically reading this manuscript.

**Grant Support:** Supported by NIH grants K01DK084205 (D.E. Frigo), P30EY007551 (A.R. Burns), R00CA125937 (L. Xin), P30CA125123 (Dan L. Duncan Cancer Center Human Tissue Acquisition and Pathology Core), DoD/PCRP grant W81XWH-12-1-0204 (D.E. Frigo), CPRIT grant RP110005 (L. Xin) and grants from the Texas Emerging Technology Fund, the Golfers Against Cancer (D.E. Frigo), the Urology Care Foundation Research Scholars Program and AUA Southeastern Section (F.G. Rick).

### References

1. Warburg O. On the origin of cancer cells. *Science*. 1956; 123:309–314. [PubMed: 13298683]
2. Hanahan D, Weinberg RA. Hallmarks of cancer: the next generation. *Cell*. 2011; 144:646–674. [PubMed: 21376230]
3. Ertel A, Tsirigos A, Whitaker-Menezes D, Birbe RC, Pavlides S, Martinez-Outschoorn UE, et al. Is cancer a metabolic rebellion against host aging? In the quest for immortality, tumor cells try to save themselves by boosting mitochondrial metabolism. *Cell Cycle*. 2012; 11:253–263. [PubMed: 22234241]
4. DeBerardinis RJ, Lum JJ, Hatzivassiliou G, Thompson CB. The biology of cancer: metabolic reprogramming fuels cell growth and proliferation. *Cell Metab*. 2008; 7:11–20. [PubMed: 18177721]
5. Dakubo GD, Parr RL, Costello LC, Franklin RB, Thayer RE. Altered metabolism and mitochondrial genome in prostate cancer. *J Clin Pathol*. 2006; 59:10–16. [PubMed: 16394275]
6. Costello LC, Franklin RB, Feng P. Mitochondrial function, zinc, and intermediary metabolism relationships in normal prostate and prostate cancer. *Mitochondrion*. 2005; 5:143–153. [PubMed: 16050980]
7. Bhalla K, Hwang BJ, Dewi RE, Ou L, Twaddel W, Fang HB, et al. PGC1 $\alpha$  promotes tumor growth by inducing gene expression programs supporting lipogenesis. *Cancer Res*. 2011; 71:6888–6898. [PubMed: 21914785]

8. Skrtic M, Sriskanthadevan S, Jhas B, Gebbia M, Wang X, Wang Z, et al. Inhibition of mitochondrial translation as a therapeutic strategy for human acute myeloid leukemia. *Cancer Cell*. 2011; 20:674–688. [PubMed: 22094260]
9. Guo JY, Chen HY, Mathew R, Fan J, Strohecker AM, Karsli-Uzunbas G, et al. Activated Ras requires autophagy to maintain oxidative metabolism and tumorigenesis. *Genes Dev*. 2011; 25:460–470. [PubMed: 21317241]
10. Xiao D, Powolny AA, Moura MB, Kelley EE, Bommareddy A, Kim SH, et al. Phenethyl isothiocyanate inhibits oxidative phosphorylation to trigger reactive oxygen species-mediated death of human prostate cancer cells. *J Biol Chem*. 2010; 285:26558–26569. [PubMed: 20571029]
11. Chang CY, Kazmin D, Jasper JS, Kunder R, Zuercher WJ, McDonnell DP. The metabolic regulator ERRalpha, a downstream target of HER2/IGF-1R, as a therapeutic target in breast cancer. *Cancer Cell*. 2011; 20:500–510. [PubMed: 22014575]
12. Cormio A, Guerra F, Cormio G, Pesce V, Fracasso F, Loizzi V, et al. The PGC-1alpha-dependent pathway of mitochondrial biogenesis is upregulated in type I endometrial cancer. *Biochem Biophys Res Commun*. 2009; 390:1182–1185. [PubMed: 19861117]
13. Hu J, Hwang SS, Liesa M, Gan B, Sahin E, Jaskelioff M, et al. Antitelomerase therapy provokes ALT and mitochondrial adaptive mechanisms in cancer. *Cell*. 2012; 148:651–663. [PubMed: 22341440]
14. Ramanathan A, Wang C, Schreiber SL. Perturbational profiling of a cell-line model of tumorigenesis by using metabolic measurements. *Proc Natl Acad Sci U S A*. 2005; 102:5992–5997. [PubMed: 15840712]
15. Stoss O, Werther M, Zielinski D, Middel P, Jost N, Ruschoff J, et al. Transcriptional profiling of transurethral resection samples provides insight into molecular mechanisms of hormone refractory prostate cancer. *Prostate Cancer Prostatic Dis*. 2008; 11:166–172. [PubMed: 17646850]
16. Whitaker-Menezes D, Martinez-Outschoorn UE, Flomenberg N, Birbe RC, Witkiewicz AK, Howell A, et al. Hyperactivation of oxidative mitochondrial metabolism in epithelial cancer cells in situ: visualizing the therapeutic effects of metformin in tumor tissue. *Cell Cycle*. 2011; 10:4047–4064. [PubMed: 22134189]
17. Yang S, Wang X, Contino G, Liesa M, Sahin E, Ying H, et al. Pancreatic cancers require autophagy for tumor growth. *Genes Dev*. 2011; 25:717–729. [PubMed: 21406549]
18. Oyama N, Miller TR, Dehdashti F, Siegel BA, Fischer KC, Michalski JM, et al. 11C-acetate PET imaging of prostate cancer: detection of recurrent disease at PSA relapse. *J Nucl Med*. 2003; 44:549–555. [PubMed: 12679398]
19. Hofer C, Laubenbacher C, Block T, Breul J, Hartung R, Schwaiger M. Fluorine-18-fluorodeoxyglucose positron emission tomography is useless for the detection of local recurrence after radical prostatectomy. *Eur Urol*. 1999; 36:31–35. [PubMed: 10364652]
20. Pillarsetty N, Punzalan B, Larson SM. 2-18F-Fluoropropionic acid as a PET imaging agent for prostate cancer. *J Nucl Med*. 2009; 50:1709–1714. [PubMed: 19759108]
21. Yu EY, Muzi M, Hackenbracht JA, Rezvani BB, Link JM, Montgomery RB, et al. C11-acetate and F-18 FDG PET for men with prostate cancer bone metastases: relative findings and response to therapy. *Clin Nucl Med*. 2011; 36:192–198. [PubMed: 21285676]
22. Taylor BS, Schultz N, Hieronymus H, Gopalan A, Xiao Y, Carver BS, et al. Integrative genomic profiling of human prostate cancer. *Cancer Cell*. 2010; 18:11–22. [PubMed: 20579941]
23. Knudsen KE, Scher HI. Starving the addiction: new opportunities for durable suppression of AR signaling in prostate cancer. *Clin Cancer Res*. 2009; 15:4792–4798. [PubMed: 19638458]
24. Chen CD, Welsbie DS, Tran C, Baek SH, Chen R, Vessella R, et al. Molecular determinants of resistance to antiandrogen therapy. *Nat Med*. 2004; 10:33–39. [PubMed: 14702632]
25. Frigo DE, Howe MK, Wittmann BM, Brunner AM, Cushman I, Wang Q, et al. CaM kinase kinase beta-mediated activation of the growth regulatory kinase AMPK is required for androgen-dependent migration of prostate cancer cells. *Cancer Res*. 2011; 71:528–537. [PubMed: 21098087]
26. Karacosta LG, Foster BA, Azabdaftari G, Feliciano DM, Edelman AM. A regulatory feedback loop between Ca<sup>2+</sup>/calmodulin-dependent protein kinase kinase 2 (CaMKK2) and the androgen receptor in prostate cancer progression. *J Biol Chem*. 2012; 287:24832–24843. [PubMed: 22654108]

27. Massie CE, Lynch A, Ramos-Montoya A, Boren J, Stark R, Fazli L, et al. The androgen receptor fuels prostate cancer by regulating central metabolism and biosynthesis. *Embo J.* 2011; 30:2719–2733. [PubMed: 21602788]
28. Park HU, Suy S, Danner M, Dailey V, Zhang Y, Li H, et al. AMP-activated protein kinase promotes human prostate cancer cell growth and survival. *Mol Cancer Ther.* 2009; 8:733–741. [PubMed: 19372545]
29. Jung SN, Park IJ, Kim MJ, Kang I, Choe W, Kim SS, et al. Down-regulation of AMP-activated protein kinase sensitizes DU145 carcinoma to Fas-induced apoptosis via c-FLIP degradation. *Exp Cell Res.* 2009; 315:2433–2441. [PubMed: 19477172]
30. Jeon SM, Chandel NS, Hay N. AMPK regulates NADPH homeostasis to promote tumour cell survival during energy stress. *Nature.* 2012; 485:661–665. [PubMed: 22660331]
31. Laderoute KR, Amin K, Calaoagan JM, Knapp M, Le T, Orduna J, et al. 5'-AMP-activated protein kinase (AMPK) is induced by low-oxygen and glucose deprivation conditions found in solid-tumor microenvironments. *Mol Cell Biol.* 2006; 26:5336–5347. [PubMed: 16809770]
32. Wang J, Cai Y, Shao LJ, Siddiqui J, Palanisamy N, Li R, et al. Activation of NF- $\kappa$ B by TMPRSS2/ERG Fusion Isoforms through Toll-Like Receptor-4. *Cancer Res.* 2011; 71:1325–1333. [PubMed: 21169414]
33. Agoulnik IU, Vaid A, Bingman WE 3rd, Erdeme H, Frolov A, Smith CL, et al. Role of SRC-1 in the promotion of prostate cancer cell growth and tumor progression. *Cancer Res.* 2005; 65:7959–7967. [PubMed: 16140968]
34. Hodgson MC, Shao LJ, Frolov A, Li R, Peterson LE, Ayala G, et al. Decreased expression and androgen regulation of the tumor suppressor gene INPP4B in prostate cancer. *Cancer Res.* 2011; 71:572–582. [PubMed: 21224358]
35. Moon JS, Jin WJ, Kwak JH, Kim HJ, Yun MJ, Kim JW, et al. Androgen stimulates glycolysis for de novo lipid synthesis by increasing the activities of hexokinase 2 and 6-phosphofructo-2-kinase/fructose-2,6-bisphosphatase 2 in prostate cancer cells. *Biochem J.* 2011; 433:225–233. [PubMed: 20958264]
36. Liu Y, Zuckier LS, Ghesani NV. Dominant uptake of fatty acid over glucose by prostate cells: a potential new diagnostic and therapeutic approach. *Anticancer Res.* 2010; 30:369–374. [PubMed: 20332441]
37. Zha S, Ferdinandusse S, Hicks JL, Denis S, Dunn TA, Wanders RJ, et al. Peroxisomal branched chain fatty acid beta-oxidation pathway is upregulated in prostate cancer. *Prostate.* 2005; 63:316–323. [PubMed: 15599942]
38. Liu Y. Fatty acid oxidation is a dominant bioenergetic pathway in prostate cancer. *Prostate Cancer Prostatic Dis.* 2006; 9:230–234. [PubMed: 16683009]
39. Sreekumar A, Poisson LM, Rajendiran TM, Khan AP, Cao Q, Yu J, et al. Metabolomic profiles delineate potential role for sarcosine in prostate cancer progression. *Nature.* 2009; 457:910–914. [PubMed: 19212411]
40. Jager S, Handschin C, St-Pierre J, Spiegelman BM. AMP-activated protein kinase (AMPK) action in skeletal muscle via direct phosphorylation of PGC-1 $\alpha$ . *Proc Natl Acad Sci U S A.* 2007; 104:12017–12022. [PubMed: 17609368]
41. Berger R, Febbo PG, Majumder PK, Zhao JJ, Mukherjee S, Signoretti S, et al. Androgen-induced differentiation and tumorigenicity of human prostate epithelial cells. *Cancer Res.* 2004; 64:8867–8875. [PubMed: 15604246]
42. Rick FG, Schally AV, Block NL, Halmos G, Perez R, Fernandez JB, et al. LHRH antagonist Cetrorelix reduces prostate size and gene expression of proinflammatory cytokines and growth factors in a rat model of benign prostatic hyperplasia. *Prostate.* 2011; 71:736–747. [PubMed: 20945403]
43. Rick FG, Schally AV, Block NL, Nadji M, Szepeshazi K, Zarandi M, et al. Antagonists of growth hormone-releasing hormone (GHRH) reduce prostate size in experimental benign prostatic hyperplasia. *Proc Natl Acad Sci U S A.* 2011; 108:3755–3760. [PubMed: 21321192]
44. Wang S, Gao J, Lei Q, Rozengurt N, Pritchard C, Jiao J, et al. Prostate-specific deletion of the murine Pten tumor suppressor gene leads to metastatic prostate cancer. *Cancer Cell.* 2003; 4:209–221. [PubMed: 14522255]

45. Ellwood-Yen K, Graeber TG, Wongvipat J, Iruela-Arispe ML, Zhang J, Matusik R, et al. Myc-driven murine prostate cancer shares molecular features with human prostate tumors. *Cancer Cell*. 2003; 4:223–238. [PubMed: 14522256]
46. Varambally S, Yu J, Laxman B, Rhodes DR, Mehra R, Tomlins SA, et al. Integrative genomic and proteomic analysis of prostate cancer reveals signatures of metastatic progression. *Cancer Cell*. 2005; 8:393–406. [PubMed: 16286247]
47. Arredouani MS, Lu B, Bhasin M, Eljanne M, Yue W, Mosquera JM, et al. Identification of the transcription factor single-minded homologue 2 as a potential biomarker and immunotherapy target in prostate cancer. *Clin Cancer Res*. 2009; 15:5794–5802. [PubMed: 19737960]
48. Chandran UR, Ma C, Dhir R, Bisceglia M, Lyons-Weiler M, Liang W, et al. Gene expression profiles of prostate cancer reveal involvement of multiple molecular pathways in the metastatic process. *BMC Cancer*. 2007; 7:64. [PubMed: 17430594]
49. Liu P, Ramachandran S, Ali Seyed M, Scharer CD, Laycock N, Dalton WB, et al. Sex-determining region Y box 4 is a transforming oncogene in human prostate cancer cells. *Cancer Res*. 2006; 66:4011–4019. [PubMed: 16618720]
50. Tamura K, Furihata M, Tsunoda T, Ashida S, Takata R, Obara W, et al. Molecular features of hormone-refractory prostate cancer cells by genome-wide gene expression profiles. *Cancer Res*. 2007; 67:5117–5125. [PubMed: 17545589]
51. Ward PS, Thompson CB. Metabolic reprogramming: a cancer hallmark even warburg did not anticipate. *Cancer Cell*. 2012; 21:297–308. [PubMed: 22439925]
52. Shiota M, Yokomizo A, Tada Y, Inokuchi J, Tatsugami K, Kuroiwa K, et al. Peroxisome proliferator-activated receptor gamma coactivator-1alpha interacts with the androgen receptor (AR) and promotes prostate cancer cell growth by activating the AR. *Mol Endocrinol*. 2010; 24:114–127. [PubMed: 19884383]
53. Marin-Valencia I, Yang C, Mashimo T, Cho S, Baek H, Yang XL, et al. Analysis of tumor metabolism reveals mitochondrial glucose oxidation in genetically diverse human glioblastomas in the mouse brain in vivo. *Cell Metab*. 2012; 15:827–837. [PubMed: 22682223]
54. Sahin E, Colla S, Liesa M, Moslehi J, Muller FL, Guo M, et al. Telomere dysfunction induces metabolic and mitochondrial compromise. *Nature*. 2011; 470:359–365. [PubMed: 21307849]
55. Ding Z, Wu CJ, Jaskelioff M, Ivanova E, Kost-Alimova M, Protopopov A, et al. Telomerase reactivation following telomere dysfunction yields murine prostate tumors with bone metastases. *Cell*. 2012; 148:896–907. [PubMed: 22341455]
56. O'Mahony F, Razandi M, Pedram A, Harvey BJ, Levin ER. Estrogen modulates metabolic pathway adaptation to available glucose in breast cancer cells. *Mol Endocrinol*. 2012; 26:2058–2070. [PubMed: 23028062]
57. Xiang X, Saha AK, Wen R, Ruderman NB, Luo Z. AMP-activated protein kinase activators can inhibit the growth of prostate cancer cells by multiple mechanisms. *Biochem Biophys Res Commun*. 2004; 321:161–167. [PubMed: 15358229]
58. Irrcher I, Ljubovic V, Kirwan AF, Hood DA. AMP-activated protein kinase-regulated activation of the PGC-1alpha promoter in skeletal muscle cells. *PLoS One*. 2008; 3:e3614. [PubMed: 18974883]
59. Klimcakova E, Chenard V, McGuirk S, Germain D, Avizonis D, Muller WJ, et al. PGC-1alpha promotes the growth of ErbB2/Neu-induced mammary tumors by regulating nutrient supply. *Cancer Res*. 2012; 72:1538–1546. [PubMed: 22266114]
60. Koves TR, Ussher JR, Noland RC, Slentz D, Mosedale M, Ilkayeva O, et al. Mitochondrial overload and incomplete fatty acid oxidation contribute to skeletal muscle insulin resistance. *Cell Metab*. 2008; 7:45–56. [PubMed: 18177724]
61. Jin C, McKeehan K, Wang F. Transgenic mouse with high Cre recombinase activity in all prostate lobes, seminal vesicle, and ductus deferens. *Prostate*. 2003; 57:160–164. [PubMed: 12949940]
62. Zhang B, Chen H, Zhang L, Dakhova O, Zhang Y, Lewis MT, et al. A dosage-dependent pleiotropic role of Dicer in prostate cancer growth and metastasis. *Oncogene*. 2013



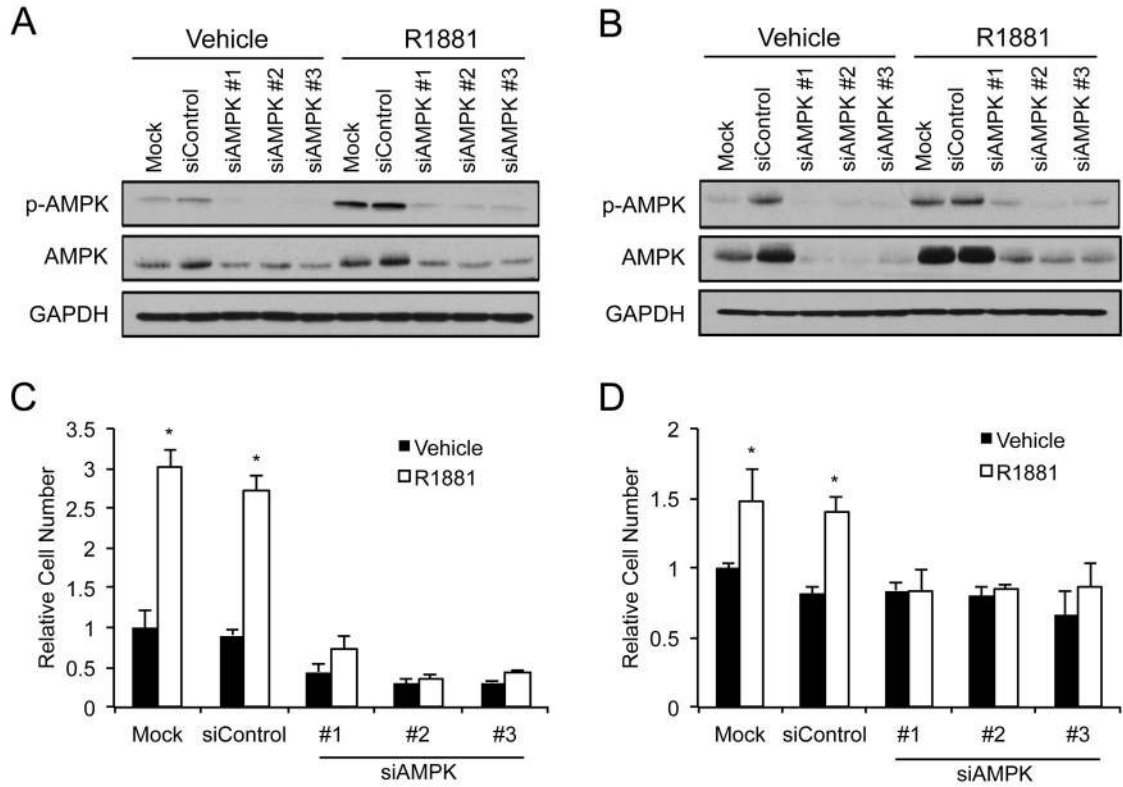


**Figure 1.** AMPK is required for androgen-mediated prostate cancer cell growth. A and B, LNCaP (A) or VCaP (B) cells were transfected with mock or siRNAs targeting a  $\beta$ -lactamase negative control (siControl) or AMPK $\alpha$ 1 (#1-3). The following day, cells were treated for 72 hours  $\pm$  10 nM R1881 (synthetic androgen). Whole cell extracts were subjected to Western blot analysis using GAPDH as a loading control. C and D, LNCaP (C) and VCaP (D) cells were transfected the same as in A and B and then treated for 7 days  $\pm$  R1881. Cells were then lysed and the relative number of cells was quantified using a fluorescent DNA-binding dye. Results are expressed as mean relative cell number + SE (n = 3). \*, significant changes from vehicle-treated cells.

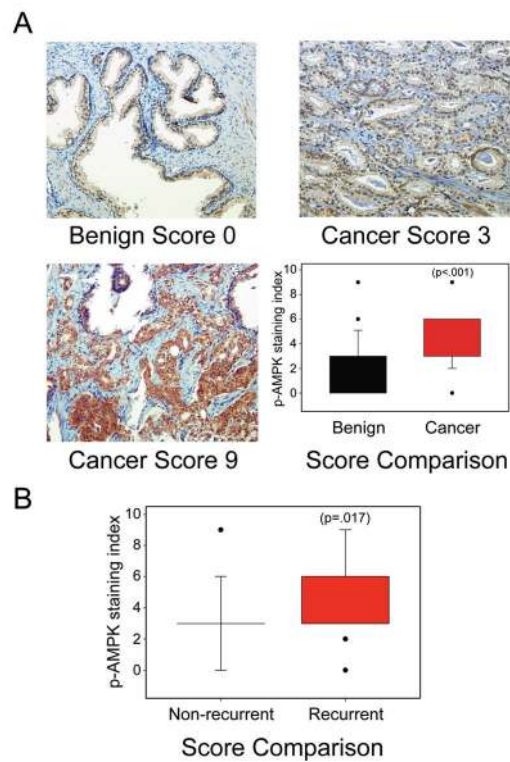


**Figure 2.**

Phosphorylated/Activated AMPK correlates with clinical prostate cancer progression. A, examples of IHC with anti-phospho-AMPK antibody (Thr172). The staining index for benign and cancer epithelial cells is indicated under each figure. Original magnification: 100X. Box plot of staining index of prostate cancer ( $n = 61$ ) and benign tissues ( $n = 65$ ) is also shown. The difference in staining index was highly statistically significant ( $p < .001$ , Mann-Whitney). B, comparison of staining index of non-recurrent ( $n = 29$ ) and recurrent ( $n = 32$ ) tumors following radical prostatectomy. Staining was significantly higher in the recurrent group ( $p = .017$ , Mann-Whitney).

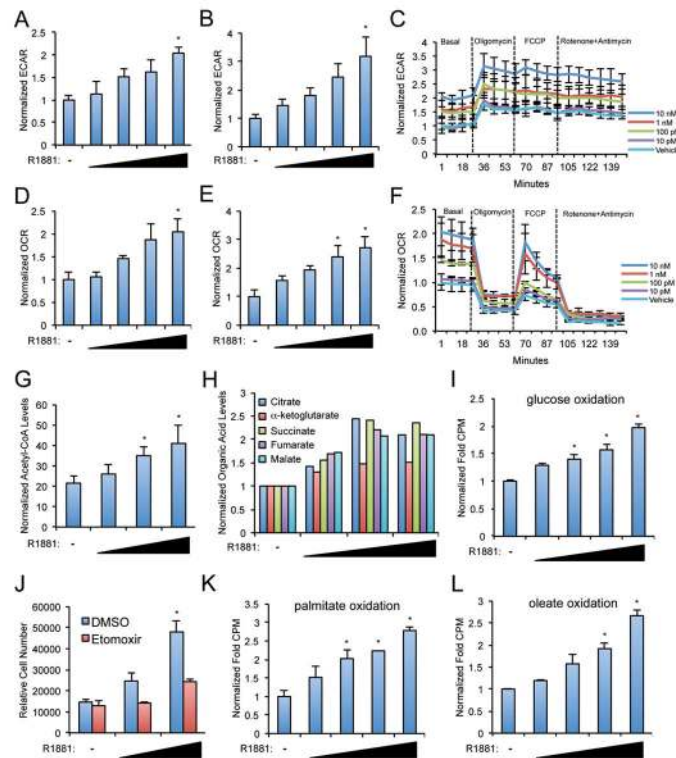


**Figure 3.**

Androgens promote glycolysis and OXPHOS in prostate cancer cells. A and B, LNCaP (A) or VCaP (B) cells were treated for 72 hours with increasing concentrations of R1881 (0, 0.01, 0.1, 1, and 10 nM). Extracellular acidification rates (ECARs) were then measured using a Seahorse XF Analyzer and values were normalized to cell numbers. Results are expressed as ECAR normalized to cell numbers + SE (n = 3). C, LNCaP cells were treated and analyzed for ECAR as in A but were also tested for effects on ECAR in the sequential presence of oligomycin, FCCP and a combination of rotenone and antimycin A. D and E, LNCaP (D) and VCaP (E) cells were treated the same as in A and B. At the same time ECAR rates were being measured, simultaneous oxygen consumption rates (OCRs) were measured and normalized the same as in A and B. F, LNCaP cells were treated and analyzed for OCR as in D but were also tested for effects on OCR in the sequential presence of oligomycin, FCCP and a combination of rotenone and antimycin A. G, LNCaP cells were treated for 72 hours with increasing doses of R1881 (0, 0.1, 1, and 10 nM). Acetyl-CoA levels were then measured using MS/MS and normalized to total protein. Results are expressed as acetyl-CoA levels normalized to total protein + SE (n = 3). H, LNCaP cells were treated as in G. TCA cycle intermediate levels were then measured using GC/MS and normalized to total protein. Results are expressed as metabolite levels normalized to total protein + SE (n = 2). I, LNCaP cells were treated as in A and then incubated with  $^{14}\text{C}$ -labeled glucose and subjected to a  $\text{CO}_2$  trap assay to measure complete glucose oxidation and normalized to cell numbers. Results are expressed as fold counts per minute (CPM) normalized to cell numbers + SE (n = 3). J, LNCaP cells were cotreated for 7 days with increasing doses of R1881 in the presence of vehicle (DMSO) or the  $\beta$ -oxidation inhibitor etomoxir (100  $\mu\text{M}$ ). Relative cell numbers were then determined as in Fig. 1. K and L,

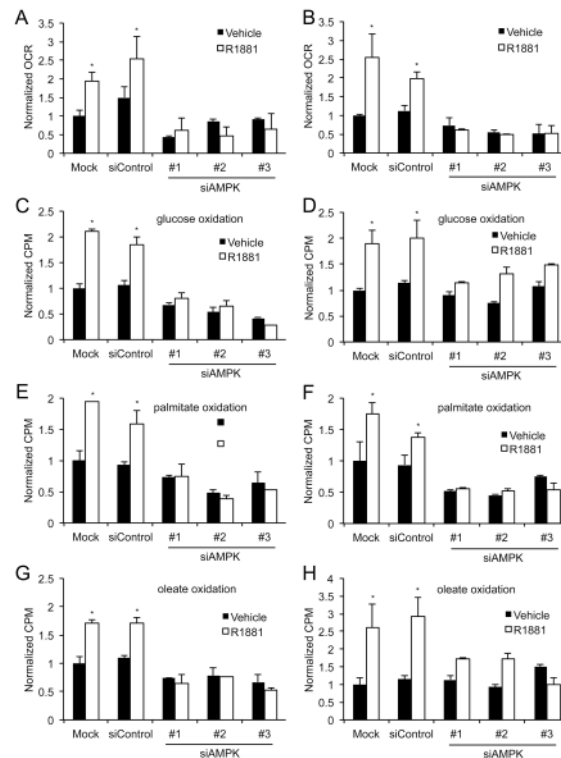
LNCaP cells were treated and subjected to a CO<sub>2</sub> trap assay the same as in I, but using <sup>14</sup>C-labeled palmitate (K) or oleate (L) to quantitate the levels of fatty acid oxidation. \*, significant changes from vehicle-treated cells.

Author Manuscript

Author Manuscript

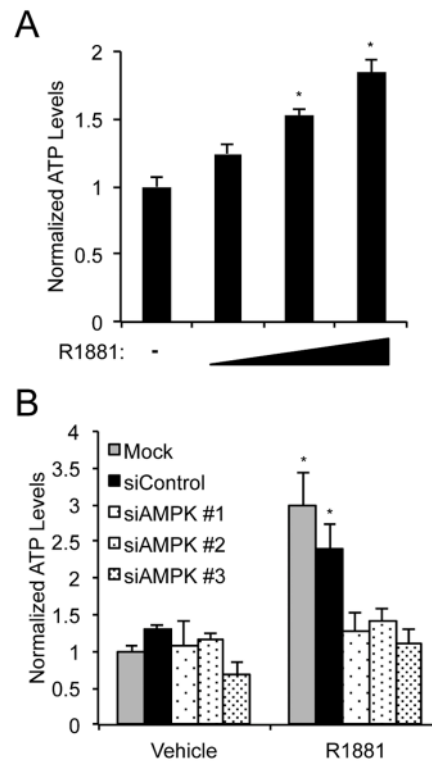
Author Manuscript

Author Manuscript



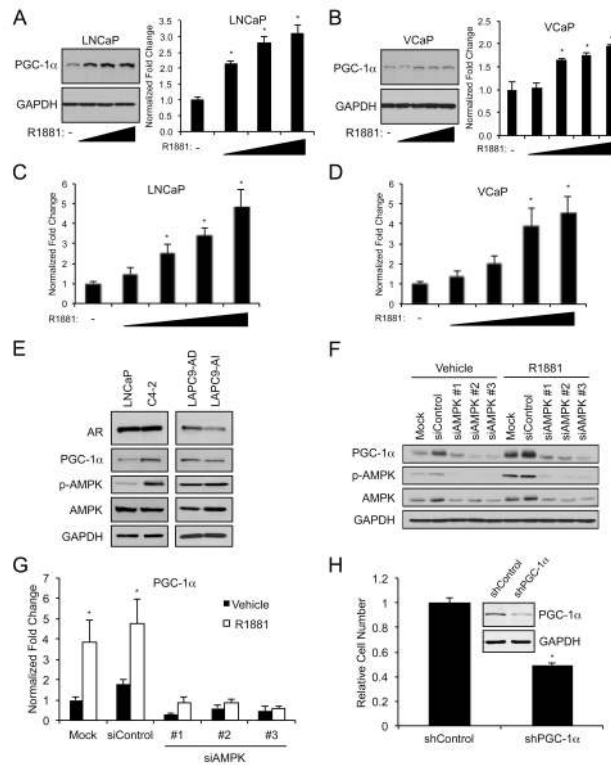
**Figure 4.**

Androgen-mediated OXPHOS requires AMPK. A and B, LNCaP (A) or VCaP (B) cells were transfected and treated as in Figs. 1A and B. OCRs were then measured using the Seahorse Analyzer and normalized to cell numbers as described in Fig. 3. C and D, LNCaP (C, E, G) or VCaP (D, F, H) cells were transfected and treated as described in A and B. Oxidation of radiolabeled glucose (C and D), palmitate (E and F) and oleate (G and H) were then measured using CO<sub>2</sub> trap assays and normalized to cell numbers as in Fig. 3. \*, significant changes from vehicle-treated cells.

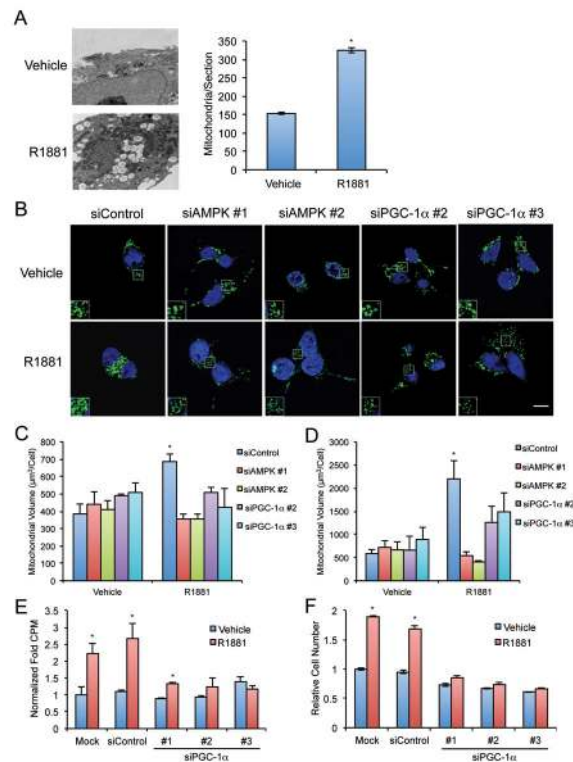


**Figure 5.**

Androgens increase intracellular ATP levels through AMPK. A, LNCaP cells were treated the same as in Fig. 3G. ATP levels were then quantitated using a luciferase-based assay and data were normalized to cell numbers. Results are expressed as relative ATP levels normalized to cell numbers + SE (n = 3). B, cells were transfected and treated as in Fig. 1A. ATP levels were then quantitated and normalized as in A. \*, significant changes from vehicle-treated cells.

**Figure 6.**

AR-AMPK signaling increases PGC-1 $\alpha$  levels. A-D, prostate cancer cells were treated with increasing concentrations of R1881 for 72 hours. A left, representative LNCaP Western blots following treatment (0, 0.1, 1 and 10 nM R1881). A right, LNCaP immunoblot densitometry values. PGC-1 $\alpha$  levels were normalized to GAPDH (n = 4). B left, representative VCaP Western blots following treatment (0, 0.01, 0.1, 1 and 10 nM R1881). B right, VCaP immunoblot densitometry values. PGC-1 $\alpha$  levels were normalized to GAPDH (n = 4). C and D, LNCaP (C) and VCaP (D) cells treated for 72 hours with 0, 0.01, 0.1, 1 or 10 nM R1881. After treatment, cells were lysed and RNA was isolated and reverse transcribed. The expression of PGC-1 $\alpha$  was assessed using qPCR (n = 3). E, cell/tumor lysates from untreated parental LNCaP and CRPC-derivative C4-2 cells or LAPC9-derived androgen-dependent (LAPC9-AD) and CRPC (LAPC9-AI) tumor xenografts were subjected to Western blot analysis. F and G, LNCaP cells were transfected and treated as described in Fig. 1A. Cells were then subjected to immunoblot (F) or qPCR (G) analysis (n = 3). Densitometry values for F are presented in Supplementary Fig. S8B. \*, significant changes from vehicle-treated cells. H, C4-2 cells stably expressing shRNAs targeting either scramble control (shControl) or PGC-1 $\alpha$  (shPGC-1 $\alpha$ ) were subjected to a 3-day cell growth/viability assay. Inset, Western blot control demonstrating PGC-1 $\alpha$  stable knockdown. \*, significant change from shControl cells.

**Figure 7.**

AR-AMPK signaling increases PGC-1 $\alpha$ -mediated mitochondrial biogenesis, OXPHOS and cell growth. A, LNCaP cells were treated  $\pm$  10 nM R1881 for 72 hours and then subjected to TEM analysis. Shown are representative images (left) and results from blinded scoring of mitochondrial numbers/section (right). B-D, VCaP (Figs. 7B and C) and LNCaP (Fig. 7D and Supplementary Fig. S10) cells were transfected with indicated siRNAs and treated as in Figs. 1A and B. Mitochondrial volume was then assessed using fluorescence confocal microscopy and subsequent image analysis. Shown are representative images (Fig. 7B and Supplementary Fig. S10) and quantitated morphometric analysis (Figs. 7C and D). Scale bar, 10  $\mu$ m. E, LNCaP cells were transfected with indicated siRNAs and treated as described in D. Oxidation of radiolabeled glucose was then measured using a CO<sub>2</sub> trap assay and normalized to cell numbers as in Fig. 4. \*, significant changes from vehicle-treated cells. F, LNCaP cells were transfected as in E and then treated for 7 days  $\pm$  R1881. Relative cell numbers were determined using the assay described in Fig. 1. \*, significant changes from vehicle-treated cells.



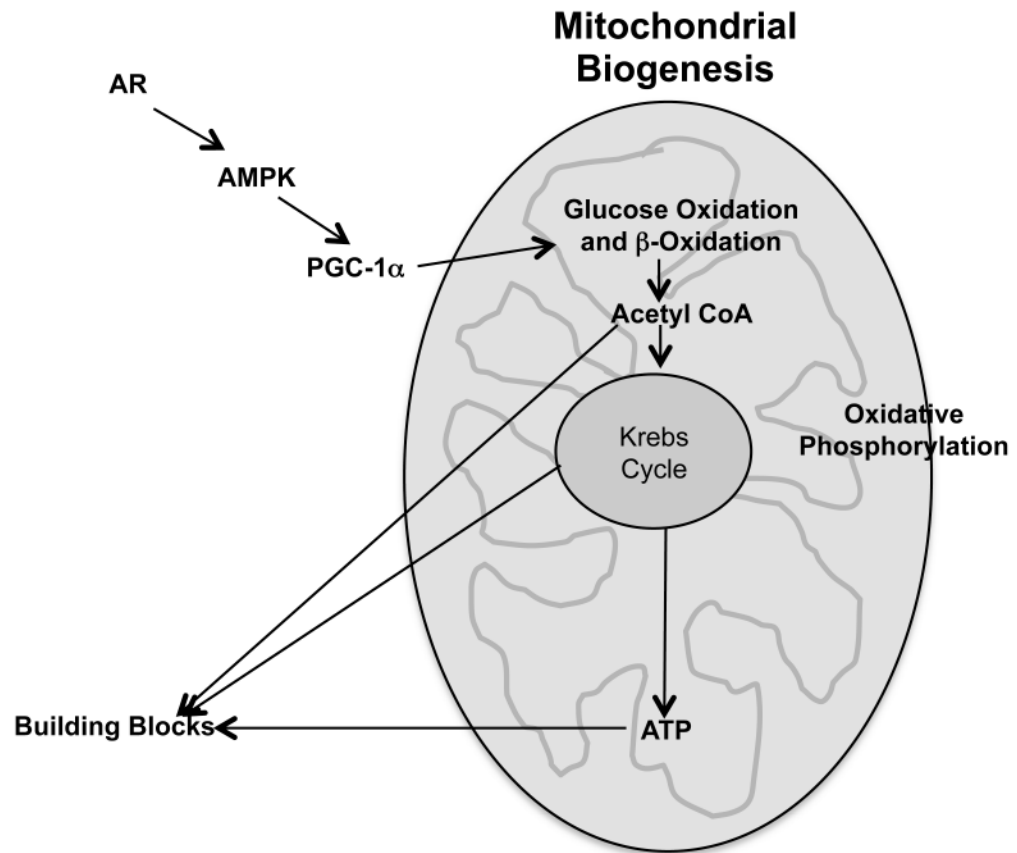


**Figure 8.** Proposed model of the AR-AMPK-PGC-1 $\alpha$  signaling axis. Androgens, through AR, increase AMPK activity. AMPK then potentiates PGC-1 $\alpha$ . Increased PGC-1 $\alpha$  can then promote mitochondria biogenesis and function.